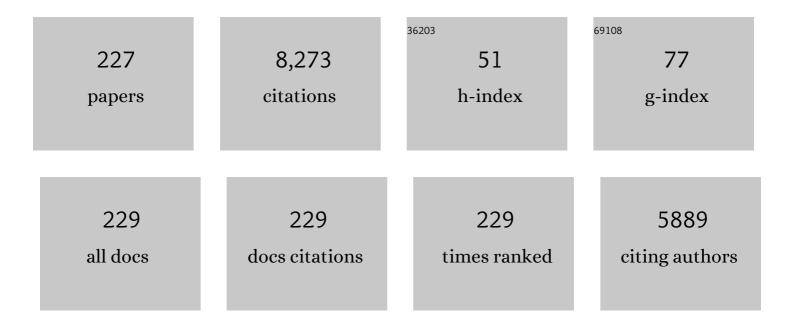
List of Publications by Year in descending order

Source: https://exaly.com/author-pdf/3490188/publications.pdf Version: 2024-02-01



ΜΑΩΝΗς ΟΠΑΩΝ

#	Article	IF	CITATIONS
1	Morphology effects on electrocatalysis of anodic water splitting on nickel (II) oxide. Microporous and Mesoporous Materials, 2022, 333, 111734.	2.2	17
2	Microstructural influence of the thermal behavior of arc deposited TiAlN coatings with high aluminum content. Journal of Alloys and Compounds, 2021, 854, 157205.	2.8	17
3	Effect of nitrogen vacancies on the growth, dislocation structure, and decomposition of single crystal epitaxial (Ti1-xAlx)Ny thin films. Acta Materialia, 2021, 203, 116509.	3.8	18
4	Temperature-dependent elastic properties of binary and multicomponent high-entropy refractory carbides. Materials and Design, 2021, 204, 109634.	3.3	26
5	Influence of pulsed-substrate bias duty cycle on the microstructure and defects of cathodic arc-deposited Ti1-xAlxN coatings. Surface and Coatings Technology, 2021, 419, 127295.	2.2	11
6	A shelf-life study of silica- and carbon-based mesoporous materials. Journal of Industrial and Engineering Chemistry, 2021, 101, 205-213.	2.9	10
7	Influence of Si content on phase stability and mechanical properties of TiAlSiN films grown by AlSi-HiPIMS/Ti-DCMS co-sputtering. Surface and Coatings Technology, 2021, 427, 127661.	2.2	22
8	Thermal degradation of TiN and TiAlN coatings during rapid laser treatment. Surface and Coatings Technology, 2021, 422, 127517.	2.2	9
9	Crater wear mechanism of TiAlN coatings during high-speed metal turning. Wear, 2021, 484-485, 204016.	1.5	5
10	Thermally induced structural evolution and age-hardening of polycrystalline V1–xMoxN (xÂâ‰^Â0.4) thin films. Surface and Coatings Technology, 2021, 405, 126723.	2.2	11
11	Spectroscopic investigation on the near-substrate plasma characteristics of chromium HiPIMS in low density discharge mode. Plasma Sources Science and Technology, 2020, 29, 015013.	1.3	12
12	3D FIB/FESEM tomography of grinding-induced damage in WC-Co cemented carbides. Procedia CIRP, 2020, 87, 385-390.	1.0	8
13	High Si content TiSiN films with superior oxidation resistance. Surface and Coatings Technology, 2020, 398, 126087.	2.2	30
14	Effect of varying N ₂ pressure on DC arc plasma properties and microstructure of TiAlN coatings. Plasma Sources Science and Technology, 2020, 29, 095015.	1.3	4
15	xmins:mml="http://www.w3.org/1998/Math/MathML`> <mml:mrow><mml:mi mathvariant="normal">T<mml:msub><mml:mi mathvariant="normal">i<mml:mrow><mml:mn>1</mml:mn><mml:mo>â^²</mml:mo><mml:mi>xIntelfacebondingrofil%mnl:mathni><mml:msub><mml:mi< td=""><td>nml:סוּסּ <td>nmlu2nrow><</td></td></mml:mi<></mml:msub></mml:mi></mml:mrow></mml:mi </mml:msub></mml:mi </mml:mrow>	nml :סוּסּ <td>nmlu2nrow><</td>	nmlu2nrow><
16	xmlns:mml="http://www.w3.org/1998/Math/MathML"> <mml:mrow><mml:mim mathvariant="normal">Z<mml:msub><mml:mi mathvariant="normal">z<mml:mrow><mml:mn>1</mml:mn><mml:mo>â^'</mml:mo><mml:mi>xmathvariant="normal">A</mml:mi><mml:msub><mml:mi mathvariant="normal">I<mml:msub><mml:mi< td=""><td>nml:m8><td>nmbmrow><!--</td--></td></td></mml:mi<></mml:msub></mml:mi </mml:msub></mml:mrow></mml:mi </mml:msub></mml:mim </mml:mrow>	nml :m8 > <td>nmbmrow><!--</td--></td>	nm b mrow> </td
17	mathvariant= normal >ix <mml:mi mathvariant="normal">N X-ray photoelectron spectroscopy studies of Ti1-Al N (0â€â‰≇€¯x â‰≇€¯0.83) high-temperature oxidation: crucial role of Al concentration. Surface and Coatings Technology, 2019, 374, 923-934.</mml:mi 	The _{2.2}	64
18	Growth and high temperature decomposition of epitaxial metastable wurtzite (Ti1-x,Alx)N(0001) thin films. Thin Solid Films, 2019, 688, 137414.	0.8	8

#	Article	IF	CITATIONS
19	A custom built lathe designed for <i>in operando</i> high-energy x-ray studies at industrially relevant cutting parameters. Review of Scientific Instruments, 2019, 90, .	0.6	3
20	Dislocation structure and microstrain evolution during spinodal decomposition of reactive magnetron sputtered heteroepixatial c-(Ti0.37,Al0.63)N/c-TiN films grown on MgO(001) and (111) substrates. Journal of Applied Physics, 2019, 125, .	1.1	12
21	Impact of the morphological and chemical properties of copper-zirconium-SBA-15 catalysts on the conversion and selectivity in carbon dioxide hydrogenation. Journal of Colloid and Interface Science, 2019, 546, 163-173.	5.0	17
22	Eutectic modification by ternary compound cluster formation in Al-Si alloys. Scientific Reports, 2019, 9, 5506.	1.6	26
23	Growth and Functionalization of Particle-Based Mesoporous Silica Films and Their Usage in Catalysis. Nanomaterials, 2019, 9, 562.	1.9	9
24	The Effect of Cathodic Arc Guiding Magnetic Field on the Growth of (Ti0.36Al0.64)N Coatings. Coatings, 2019, 9, 660.	1.2	6
25	Decomposition routes and strain evolution in arc deposited TiZrAlN coatings. Journal of Alloys and Compounds, 2019, 779, 261-269.	2.8	6
26	The effect of nitrogen vacancies on initial wear in arc deposited (Ti0.52,Al0.48)Ny, (yâ€<â€1) coatings during machining. Surface and Coatings Technology, 2019, 358, 452-460.	2.2	11
27	Characterization of DLC coatings over nitrided stainless steel with and without nitriding pre-treatment using annealing cycles. Journal of Materials Research and Technology, 2019, 8, 1653-1662.	2.6	10
28	Effect of work function and cohesive energy of the constituent phases of Ti-50†at.% Al cathode during arc deposition of Ti-Al-N coatings. Surface and Coatings Technology, 2019, 357, 393-401.	2.2	8
29	Phase Selective Sample Preparation of Al-Si alloys for Atom Probe Tomography. Praktische Metallographie/Practical Metallography, 2019, 56, 76-90.	0.1	2
30	Implementation of advanced characterisation techniques for assessment of grinding effects on the surface integrity of WC–Co cemented carbides. Powder Metallurgy, 2018, 61, 100-105.	0.9	2
31	Thermal expansion of quaternary nitride coatings. Journal of Physics Condensed Matter, 2018, 30, 135901.	0.7	5
32	Enhanced thermal stability and fracture toughness of TiAlN coatings by Cr, Nb and V-alloying. Surface and Coatings Technology, 2018, 342, 85-93.	2.2	40
33	Time evolution of the CO2 hydrogenation to fuels over Cu-Zr-SBA-15 catalysts. Journal of Catalysis, 2018, 362, 55-64.	3.1	19
34	High temperature thermodynamics of spinodal decomposition in arc deposited TixNbyAlzN coatings. Materials and Design, 2018, 150, 165-170.	3.3	7
35	Nanofibrillated Celluloseâ€Based Electrolyte and Electrode for Paperâ€Based Supercapacitors. Advanced Sustainable Systems, 2018, 2, 1700121.	2.7	38
36	Formation of block-copolymer-templated mesoporous silica. Journal of Colloid and Interface Science, 2018, 521, 183-189.	5.0	20

#	Article	IF	CITATIONS
37	Non-equilibrium vacancy formation energies in metastable alloys — A case study ofÂTi0.5Al0.5N. Materials and Design, 2017, 114, 484-493.	3.3	13
38	Mesoporous silica and carbon based catalysts for esterification and biodiesel fabrication—The effect of matrix surface composition and porosity. Applied Catalysis A: General, 2017, 533, 49-58.	2.2	40
39	Systematic ab initio investigation of the elastic modulus in quaternary transition metal nitride alloys and their coherent multilayers. Acta Materialia, 2017, 127, 124-132.	3.8	44
40	Solid state formation of Ti4AlN3 in cathodic arc deposited (Ti1â^'xAlx)Ny alloys. Acta Materialia, 2017, 129, 268-277.	3.8	18
41	Mechanical strength of ground WC-Co cemented carbides after coating deposition. Materials Science & Engineering A: Structural Materials: Properties, Microstructure and Processing, 2017, 689, 72-77.	2.6	16
42	Temperature induced superhard CrB 2 coatings with preferred (001) orientation deposited by DC magnetron sputtering technique. Surface and Coatings Technology, 2017, 322, 134-140.	2.2	19
43	Exploring the high entropy alloy concept in (AlTiVNbCr)N. Thin Solid Films, 2017, 636, 346-352.	0.8	27
44	Thermal and mechanical stability of wurtzite-ZrAlN/cubic-TiN and wurtzite-ZrAlN/cubic-ZrN multilayers. Surface and Coatings Technology, 2017, 324, 328-337.	2.2	8
45	Effects of nitrogen vacancies on phase stability and mechanical properties of arc deposited (Ti 0.52 Al) Tj ETQq1	1 0.78431	4 <u>f</u> gBT /Over
46	Discharge state transition and cathode fall thickness evolution during chromium HiPIMS discharge. Physics of Plasmas, 2017, 24, .	0.7	9
47	Enhanced thermal stability and mechanical properties of nitrogen deficient titanium aluminum nitride (Ti0.54Al0.46Ny) thin films by tuning the applied negative bias voltage. Journal of Applied Physics, 2017, 122, .	1.1	17
48	Grinding-induced metallurgical alterations in the binder phase of WC-Co cemented carbides. Materials Characterization, 2017, 134, 302-310.	1.9	24
49	Synthesis of a Cu-infiltrated Zr-doped SBA-15 catalyst for CO ₂ hydrogenation into methanol and dimethyl ether. Physical Chemistry Chemical Physics, 2017, 19, 19139-19149.	1.3	23
50	Morphology and microstructure evolution of Ti-50 at.% Al cathodes during cathodic arc deposition of Ti-Al-N coatings. Journal of Applied Physics, 2017, 121, 245309.	1.1	11
51	Effects of decomposition route and microstructure on h-AlN formation rate in TiCrAlN alloys. Journal of Alloys and Compounds, 2017, 691, 1024-1032.	2.8	9
52	Carbon Based Coatings Deposited on Nitrided Stainless Steel: Study of Thermal Degradation. Minerals, Metals and Materials Series, 2017, , 57-66.	0.3	0
53	Shape engineering boosts antibacterial activity of chitosan coated mesoporous silica nanoparticle doped with silver: a mechanistic investigation. Journal of Materials Chemistry B, 2016, 4, 3292-3304.	2.9	50
54	Cluster formation at the Si/liquid interface in Sr and Na modified Al–Si alloys. Scripta Materialia, 2016, 117, 16-19.	2.6	74

#	Article	IF	CITATIONS
55	Growth and thermal stability of TiN/ZrAlN: Effect of internal interfaces. Acta Materialia, 2016, 121, 396-406.	3.8	44
56	Impact of anharmonic effects on the phase stability, thermal transport, and electronic properties of AlN. Physical Review B, 2016, 94, .	1.1	20
57	Thermally Induced Surface Integrity Changes of Ground WC-Co Hardmetals. Procedia CIRP, 2016, 45, 91-94.	1.0	4
58	Complex 3D nanocoral like structures formed by copper nanoparticle aggregation on nanostructured zinc oxide rods. Materials Letters, 2016, 184, 127-130.	1.3	0
59	Impact of nitrogen vacancies on the high temperature behavior of (Ti1â^xAlx)Ny alloys. Acta Materialia, 2016, 119, 218-228.	3.8	41
60	Self-organized nanostructuring in Zr0.69Al0.31N thin films studied by atom probe tomography. Thin Solid Films, 2016, 615, 233-238.	0.8	10
61	Coherency effects on the mixing thermodynamics of cubic <mml:math xmlns:mml="http://www.w3.org/1998/Math/MathML"><mml:mrow><mml:msub><mml:mi>Ti</mml:mi><mml:r mathvariant="normal">N<mml:mo>/</mml:mo><mml:mi>TiN</mml:mi></mml:r </mml:msub></mml:mrow> multilayers. Physical Review B. 2016. 93</mml:math 	nrow > < mr <td>nl:mn>1th>(001)</td>	nl:mn>1th>(001)
62	Influence of microstructure and mechanical properties on the tribological behavior of reactive arc deposited Zr-Si-N coatings at room and high temperature. Surface and Coatings Technology, 2016, 304, 393-400.	2.2	10
63	Lattice Vibrations Change the Solid Solubility of an Alloy at High Temperatures. Physical Review Letters, 2016, 117, 205502.	2.9	60
64	Influence of substrate microstructure and surface finish on cracking and delamination response of TiN-coated cemented carbides. Wear, 2016, 352-353, 102-111.	1.5	9
65	Thermal stability of wurtzite Zr1â^'xAlxN coatings studied by <i>in situ</i> high-energy x-ray diffraction during annealing. Journal of Applied Physics, 2015, 118, .	1.1	20
66	Industry-relevant magnetron sputtering and cathodic arc ultra-high vacuum deposition system for <i>in situ</i> x-ray diffraction studies of thin film growth using high energy synchrotron radiation. Review of Scientific Instruments, 2015, 86, 095113.	0.6	11
67	Temperature-dependent elastic properties of Tilâ^' <i>x</i> Al <i>x</i> N alloys. Applied Physics Letters, 2015, 107, .	1.5	46
68	Tuning hardness and fracture resistance of ZrN/Zr0.63Al0.37N nanoscale multilayers by stress-induced transformation toughening. Acta Materialia, 2015, 89, 22-31.	3.8	57
69	Contact damage resistance of TiN-coated hardmetals: Beneficial effects associated with substrate grinding. Surface and Coatings Technology, 2015, 275, 133-141.	2.2	13
70	Substrate surface finish effects on scratch resistance and failure mechanisms of TiN-coated hardmetals. Surface and Coatings Technology, 2015, 265, 174-184.	2.2	21
71	Special quasirandom structure method in application for advanced properties of alloys: A study on Ti 0.5 Al 0.5 N and TiN/Ti 0.5 Al 0.5 N multilayer. Computational Materials Science, 2015, 103, 194-199.	1.4	9
72	Propylsulfonic acid functionalized mesoporous silica catalysts for esterification of fatty acids. Journal of Molecular Catalysis A, 2015, 410, 253-259.	4.8	37

#	Article	IF	CITATIONS
73	Wear behavior of ZrAlN coated cutting tools during turning. Surface and Coatings Technology, 2015, 282, 180-187.	2.2	23
74	The production of porous brick material from diatomaceous earth and Brazil nut shell ash. Construction and Building Materials, 2015, 98, 257-264.	3.2	26
75	Phase-field modelling of spinodal decomposition in TiAlN including the effect of metal vacancies. Scripta Materialia, 2015, 95, 42-45.	2.6	40
76	Self-organized anisotropic (Zr1â^'Si)N nanocomposites grown by reactive sputter deposition. Acta Materialia, 2015, 82, 179-189.	3.8	27
77	Targeted delivery of a novel anticancer compound anisomelic acid using chitosan-coated porous silica nanorods for enhancing the apoptotic effect. Biomaterials Science, 2015, 3, 103-111.	2.6	34
78	Nanostructuring and coherency strain in multicomponent hard coatings. APL Materials, 2014, 2, 116104.	2.2	6
79	High temperature phase decomposition in TixZryAlzN. AIP Advances, 2014, 4, .	0.6	13
80	Anomalous epitaxial stability of (001) interfaces in ZrN/SiNx multilayers. APL Materials, 2014, 2, 046106.	2.2	10
81	Vibrational free energy and phase stability of paramagnetic and antiferromagnetic CrN from <i>ab initio</i> molecular dynamics. Physical Review B, 2014, 89, .	1.1	46
82	Single-pot synthesis of ordered mesoporous silica films with unique controllable morphology. Journal of Colloid and Interface Science, 2014, 413, 1-7.	5.0	16
83	Effects of the cathode grain size and substrate fixture movement on the evolution of arc evaporated Cr-cathodes and Cr-N coating synthesis. Journal of Vacuum Science and Technology A: Vacuum, Surfaces and Films, 2014, 32, 021515.	0.9	3
84	Structure, deformation and fracture of arc evaporated Zr–Si–N hard films. Surface and Coatings Technology, 2014, 258, 1100-1107.	2.2	31
85	High temperature phase evolution of Bolivian kaolinitic–illitic clays heated to 1250°C. Applied Clay Science, 2014, 101, 100-105.	2.6	41
86	In situ X-ray scattering study of the cubic to hexagonal transformation of AlN in Ti1â^'xAlxN. Acta Materialia, 2014, 73, 205-214.	3.8	71
87	Comparison of segregations formed in unmodified and Sr-modified Al–Si alloys studied by atom probe tomography and transmission electron microscopy. Journal of Alloys and Compounds, 2014, 611, 410-421.	2.8	59
88	Grinding Effects on Surface Integrity and Mechanical Strength of WC-Co Cemented Carbides. Procedia CIRP, 2014, 13, 257-263.	1.0	61
89	Improved metal cutting performance with bias-modulated textured Ti0.50Al0.50N multilayers. Surface and Coatings Technology, 2014, 257, 102-107.	2.2	15
90	3D Microstructure Characterization and Analysis of Al-Si Foundry Alloys at Different Length Scales. Microscopy and Microanalysis, 2014, 20, 956-957.	0.2	19

#	Article	IF	CITATIONS
91	A new approach to account for fracture aperture variability when modeling solute transport in fracture networks. Water Resources Research, 2013, 49, 2241-2252.	1.7	17
92	Tuning the Shape of Mesoporous Silica Particles by Alterations in Parameter Space: From Rods to Platelets. Langmuir, 2013, 29, 13551-13561.	1.6	44
93	Growth of hard amorphous TiAlSiN thin films by cathodic arc evaporation. Surface and Coatings Technology, 2013, 235, 376-382.	2.2	21
94	Effects of Ti alloying of AlCrN coatings on thermal stability and oxidation resistance. Thin Solid Films, 2013, 534, 394-402.	0.8	59
95	Influence of Ti–Si cathode grain size on the cathodic arc process and resulting Ti–Si–N coatings. Surface and Coatings Technology, 2013, 235, 637-647.	2.2	16
96	Anisotropy effects on microstructure and properties in decomposed arc evaporated Ti1-xAlxN coatings during metal cutting. Surface and Coatings Technology, 2013, 235, 181-185.	2.2	31
97	Growth of Gd2O3 nanoparticles inside mesoporous silica frameworks. Microporous and Mesoporous Materials, 2013, 168, 221-224.	2.2	29
98	Blind deconvolution of time-of-flight mass spectra from atom probe tomography. Ultramicroscopy, 2013, 132, 60-64.	0.8	18
99	Microstructure evolution during the isostructural decomposition of TiAlN <i>—</i> A combined <i>in-situ</i> small angle x-ray scattering and phase field study. Journal of Applied Physics, 2013, 113, .	1.1	63
100	High pressure and high temperature stabilization of cubic AlN in Ti0.60Al0.40N. Journal of Applied Physics, 2013, 113, .	1.1	34
101	Nanolabyrinthine ZrAlN thin films by self-organization of interwoven single-crystal cubic and hexagonal phases. APL Materials, 2013, 1, .	2.2	35
102	Surface directed spinodal decomposition at TiAlN/TiN interfaces. Journal of Applied Physics, 2013, 113, .	1.1	41
103	Coherency strain engineered decomposition of unstable multilayer alloys for improved thermal stability. Journal of Applied Physics, 2013, 114, .	1.1	10
104	Influence of chemical composition and deposition conditions on microstructure evolution during annealing of arc evaporated ZrAlN thin films. Journal of Vacuum Science and Technology A: Vacuum, Surfaces and Films, 2012, 30, of cubic Tikmml:math	0.9	26
105	xmins:mml="http://www.w3.org/1998/Math/MathML" display="inline"> <mml:msub><mml:mrow /><mml:mrow><mml:mn>0.5</mml:mn></mml:mrow></mml:mrow </mml:msub> Al <mml:math xmlns:mml="http://www.w3.org/1998/Math/MathML" display="inline"><mml:math>Al<mml:math /><mml:mrow><mml:mn>0.5</mml:mn></mml:mrow></mml:math </mml:math>N alloys: Dependence of</mml:math 	1.1	125
106	elastic constants on size and shape of the supercell model and their convergence. Physical Review 8, Thermal treatment and phase formation in kaolinite and illite based clays from tropical regions of Bolivia. IOP Conference Series: Materials Science and Engineering, 2012, 31, 012017.	0.3	21
107	Phase transformations in nanocomposite ZrAlN thin films during annealing. Journal of Materials Research, 2012, 27, 1716-1724.	1.2	16
108	Decomposition and phase transformation in TiCrAlN thin coatings. Journal of Vacuum Science and Technology A: Vacuum, Surfaces and Films, 2012, 30, .	0.9	44

#	Article	IF	CITATIONS
109	Auto-organizing ZrAlN/ZrAlTiN/TiN multilayers. Thin Solid Films, 2012, 520, 6451-6454.	0.8	11
110	Immobilization of lipase from Mucor miehei and Rhizopus oryzae into mesoporous silica—The effect of varied particle size and morphology. Colloids and Surfaces B: Biointerfaces, 2012, 100, 22-30.	2.5	81
111	Shape engineering vs organic modification of inorganic nanoparticles as a tool for enhancing cellular internalization. Nanoscale Research Letters, 2012, 7, 358.	3.1	61
112	Pressure and temperature effects on the decomposition of arc evaporated Ti0.6Al0.4N coatings in continuous turning. Surface and Coatings Technology, 2012, 209, 203-207.	2.2	52
113	Arc deposition of Ti–Si–C–N thin films from binary and ternary cathodes — Comparing sources of C. Surface and Coatings Technology, 2012, 213, 145-154.	2.2	15
114	Microstructural and Chemical Analysis of Agl Coatings Used as a Solid Lubricant in Electrical Sliding Contacts. Tribology Letters, 2012, 46, 187-193.	1.2	16
115	Spinodal decomposition of Ti0.33Al0.67N thin films studied by atom probe tomography. Thin Solid Films, 2012, 520, 4362-4368.	0.8	63
116	Strain evolution during spinodal decomposition of TiAlN thin films. Thin Solid Films, 2012, 520, 5542-5549.	0.8	101
117	Low temperature nanocasting of hematite nanoparticles using mesoporous silica molds. Powder Technology, 2012, 217, 269-273.	2.1	5
118	Synthesis of homogeneously dispersed cobalt nanoparticles in the pores of functionalized SBA-15 silica. Powder Technology, 2012, 221, 359-364.	2.1	18
119	Extended studies of degradation mechanisms in the refractory lining of a rotary kiln for iron ore pellet production. Journal of the European Ceramic Society, 2012, 32, 1519-1528.	2.8	41
120	Ti–Si–C–N thin films grown by reactive arc evaporation from Ti ₃ SiC ₂ cathodes. Journal of Materials Research, 2011, 26, 874-881.	1.2	19
121	Rapid Synthesis of SBA-15 Rods with Variable Lengths, Widths, and Tunable Large Pores. Langmuir, 2011, 27, 4994-4999.	1.6	72
122	Silica SBA-15 Template Assisted Synthesis of Ultrasmall and Homogeneously Sized Copper Nanoparticles. Journal of Nanoscience and Nanotechnology, 2011, 11, 3493-3498.	0.9	4
123	Phase Stability and Elasticity of TiAlN. Materials, 2011, 4, 1599-1618.	1.3	80
124	Improving thermal stability of hard coating films via a concept of multicomponent alloying. Applied Physics Letters, 2011, 99, .	1.5	95
125	Annealing of Thermally Sprayed Ti2AlC Coatings. International Journal of Applied Ceramic Technology, 2011, 8, 74-84.	1.1	36
126	The Reactivity of Ti2AlC and Ti3SiC2 with SiC Fibers and Powders up to Temperatures of 1550°C. Journal of the American Ceramic Society, 2011, 94, 1737-1743.	1.9	40

#	Article	IF	CITATIONS
127	Phase Evaluation in <scp>Al₂O₃</scp> Fiberâ€Reinforced <scp>Ti₂AlC</scp> During Sintering in the 1300°C–1500°C Temperature Range. Journal of the American Ceramic Society, 2011, 94, 3327-3334.	1.9	22
128	Synthesis of hollow silica spheres SBA-16 with large-pore diameter. Materials Letters, 2011, 65, 1066-1068.	1.3	17
129	Mesoporous silica templated zirconia nanoparticles. Journal of Nanoparticle Research, 2011, 13, 2743-2748.	0.8	5
130	Growth of single crystalline dendritic Li2SiO3 arrays from LiNO3 and mesoporous SiO2. Journal of Solid State Chemistry, 2011, 184, 1735-1739.	1.4	4
131	Layer formation by resputtering in Ti–Si–C hard coatings during large scale cathodic arc deposition. Surface and Coatings Technology, 2011, 205, 3923-3930.	2.2	83
132	Machining performance and decomposition of TiAlN/TiN multilayer coated metal cutting inserts. Surface and Coatings Technology, 2011, 205, 4005-4010.	2.2	67
133	Microstructure evolution of Ti3SiC2 compound cathodes during reactive cathodic arc evaporation. Journal of Vacuum Science and Technology A: Vacuum, Surfaces and Films, 2011, 29, 031601.	0.9	10
134	Load partitioning between single bulk grains in a two-phase duplex stainless steel during tensile loading. Acta Materialia, 2010, 58, 734-744.	3.8	49
135	Thermomechanical properties of copper–carbon nanofibre composites prepared by spark plasma sintering and hot pressing. Composites Science and Technology, 2010, 70, 2263-2268.	3.8	53
136	Age hardening in arc-evaporated ZrAlN thin films. Scripta Materialia, 2010, 62, 739-741.	2.6	37
137	Influence of synthesis temperature on morphology of SBA-16 mesoporous materials with a three-dimensional pore system. Microporous and Mesoporous Materials, 2010, 129, 106-111.	2.2	39
138	The effects on pore size and particle morphology of heptane additions to the synthesis of mesoporous silica SBA-15. Microporous and Mesoporous Materials, 2010, 133, 66-74.	2.2	58
139	Thermal stability and mechanical properties of arc evaporated ZrN/ZrAlN multilayers. Thin Solid Films, 2010, 519, 694-699.	0.8	31
140	Microstructure evolution and age hardening in (Ti,Si)(C,N) thin films deposited by cathodic arc evaporation. Thin Solid Films, 2010, 519, 1397-1403.	0.8	35
141	Microstructural characterization of alkali metal mediated high temperature reactions in mullite based refractories. Ceramics International, 2010, 36, 733-740.	2.3	30
142	Effect of heat treatment of carbon nanofibres on electroless copper deposition. Composites Science and Technology, 2010, 70, 2269-2275.	3.8	19
143	Thermally enhanced mechanical properties of arc evaporated Ti0.34Al0.66N/TiN multilayer coatings. Journal of Applied Physics, 2010, 108, .	1.1	86
144	Significant elastic anisotropy in Ti1â^'xAlxN alloys. Applied Physics Letters, 2010, 97, .	1.5	107

#	Article	IF	CITATIONS
145	Characterization of worn Ti–Si cathodes used for reactive cathodic arc evaporation. Journal of Vacuum Science and Technology A: Vacuum, Surfaces and Films, 2010, 28, 347-353.	0.9	19
146	Pressure enhancement of the isostructural cubic decomposition in Ti1â^'xAlxN. Applied Physics Letters, 2009, 95, .	1.5	67
147	<i>In situ</i> small-angle x-ray scattering study of nanostructure evolution during decomposition of arc evaporated TiAlN coatings. Applied Physics Letters, 2009, 94, .	1.5	59
148	Synthesis and characterization of large mesoporous silica SBA-15 sheets with ordered accessible 18Ânm pores. Materials Letters, 2009, 63, 2129-2131.	1.3	31
149	Load Partitioning and Strain-Induced Martensite Formation during Tensile Loading of a Metastable Austenitic Stainless Steel. Metallurgical and Materials Transactions A: Physical Metallurgy and Materials Science, 2009, 40, 1039-1048.	1.1	71
150	Degradation of Refractory Bricks Used as Thermal Insulation in Rotary Kilns for Iron Ore Pellet Production. International Journal of Applied Ceramic Technology, 2009, 6, 717-726.	1.1	16
151	Growth and characterization of electroless deposited Cu films on carbon nanofibers. Surface and Coatings Technology, 2009, 203, 3459-3464.	2.2	17
152	Fabrication of transparent yttria by HIP and the glass-encapsulation method. Journal of the European Ceramic Society, 2009, 29, 311-316.	2.8	69
153	Microwave assisted combustion synthesis of nanocrystalline yttria and its powder characteristics. Powder Technology, 2009, 191, 309-314.	2.1	92
154	Morphology influence of the oxidation kinetics of carbon nanofibers. Corrosion Science, 2009, 51, 926-930.	3.0	15
155	On the Stability of Mg Nanograins to Coarsening after Repeated Melting. Nano Letters, 2009, 9, 3082-3086.	4.5	16
156	Synthesis of nanocrystalline yttria through in-situ sulphated-combustion technique. Journal of the Ceramic Society of Japan, 2009, 117, 1065-1068.	0.5	7
157	Sintering, microstructural and mechanical characterization of combustion synthesized Y2O3 and Yb3+-Y2O3. Journal of the Ceramic Society of Japan, 2009, 117, 1258-1262.	0.5	4
158	Preparation and firing of a TiC/Si powder mixture. IOP Conference Series: Materials Science and Engineering, 2009, 5, 012016.	0.3	2
159	Comparison between slip-casting and uniaxial pressing for the fabrication of translucent yttria ceramics. Journal of Materials Science, 2008, 43, 2849-2856.	1.7	33
160	Combustion synthesis of Y2O3 and Yb–Y2O3. Journal of Materials Processing Technology, 2008, 208, 415-422.	3.1	82
161	Thermal stability, microstructure and mechanical properties of Ti1â^'xZrxN thin films. Thin Solid Films, 2008, 516, 6421-6431.	0.8	76
162	Influence of Agglomeration on the Transparency of Yttria Ceramics. Journal of the American Ceramic Society, 2008, 91, 3380-3387.	1.9	18

#	Article	IF	CITATIONS
163	Elastic strain evolution and ε-martensite formation in individual austenite grains during in situ loading of a metastable stainless steel. Materials Letters, 2008, 62, 338-340.	1.3	28
164	Regional channelized transport in fractured media with matrix diffusion and linear sorption. Water Resources Research, 2008, 44, .	1.7	15
165	Synthesis and optical properties of Yb0.6Y1.4O3 transparent ceramics. Journal of Alloys and Compounds, 2008, 464, 407-411.	2.8	17
166	Thermal decomposition products in arc evaporated TiAlN/TiN multilayers. Applied Physics Letters, 2008, 93, .	1.5	74
167	Reverse Martensitic Transformation and Resulting Microstructure in a Cold Rolled Metastable Austenitic Stainless Steel. Steel Research International, 2008, 79, 433-439.	1.0	13
168	Interface structure in superhard TiN-SiN nanolaminates and nanocomposites: Film growth experiments andab initiocalculations. Physical Review B, 2007, 75, .	1.1	142
169	Growth and characterization of TiN/SiN(001) superlattice films. Journal of Materials Research, 2007, 22, 3255-3264.	1.2	49
170	RHEED studies during growth of TiN/SiNx/TiN trilayers on MgO(001). Surface Science, 2007, 601, 2352-2356.	0.8	8
171	Alternative method to precipitation techniques for synthesizing yttrium oxide nanopowder. Powder Technology, 2007, 177, 77-82.	2.1	19
172	Comparison of two different precipitation routes leading to Yb doped Y2O3 nano-particles. Journal of the European Ceramic Society, 2007, 27, 1991-1998.	2.8	18
173	Stepwise transformation behavior of the strain-induced martensitic transformation in a metastable stainless steel. Scripta Materialia, 2007, 56, 213-216.	2.6	72
174	Effect of Drying and Dewatering on Yttria Precursors with Transient Morphology. Journal of the American Ceramic Society, 2006, 89, 3094-3100.	1.9	23
175	Comparison of relative permeability–fluid saturation–capillary pressure relations in the modelling of non-aqueous phase liquid infiltration in variably saturated, layered media. Advances in Water Resources, 2006, 29, 1705-1730.	1.7	24
176	From well-test data to input to stochastic continuum models: effect of the variable support scale of the hydraulic data. Hydrogeology Journal, 2006, 14, 1409-1422.	0.9	11
177	Evolution of Residual Strains in Metastable Austenitic Stainless Steels and the Accompanying Strain Induced Martensitic Transformation. Materials Science Forum, 2006, 524-525, 821-826.	0.3	2
178	Residual Stress Evolution during Decomposition of Ti _(1-x) Al _(x) N Coatings Using High-Energy X-Rays. Materials Science Forum, 2006, 524-525, 619-624.	0.3	2
179	Epitaxial stabilization of cubic-SiNx in TiNâ^•SiNx multilayers. Applied Physics Letters, 2006, 88, 191902.	1.5	71
180	Mechanical properties and machining performance of Ti1â^'xAlxN-coated cutting tools. Surface and Coatings Technology, 2005, 191, 384-392.	2.2	475

#	ARTICLE	IF	CITATIONS
181	Grain-to-Grain Stress Interactions in an Electrodeposited Iron Coating. Advanced Materials, 2005, 17, 1221-1226.	11.1	17
182	Determination of Grain-Orientation-Dependent Stress in Coatings. Solid State Phenomena, 2005, 105, 107-112.	0.3	0
183	Residual Stress Analysis in Both As-Deposited and Annealed CrN Coatings. Materials Science Forum, 2005, 490-491, 643-648.	0.3	3
184	Nanostructure formation during deposition of TiNâ^•SiNx nanomultilayer films by reactive dual magnetron sputtering. Journal of Applied Physics, 2005, 97, 114327.	1.1	145
185	Microstructure and thermal stability of arc-evaporated Cr–C–N coatings. Philosophical Magazine, 2004, 84, 611-630.	0.7	12
186	X-ray diffraction determination of residual stresses in functionally graded WC–Co composites. International Journal of Refractory Metals and Hard Materials, 2004, 22, 177-184.	1.7	32
187	Hardness profile measurements in functionally graded WC–Co composites. Materials Science & Engineering A: Structural Materials: Properties, Microstructure and Processing, 2004, 382, 141-149.	2.6	14
188	Magnetron sputtered W–C films with C60 as carbon source. Thin Solid Films, 2003, 444, 29-37.	0.8	60
189	Electrochemically deposited nickel membranes; process–microstructure–property relationships. Surface and Coatings Technology, 2003, 172, 79-89.	2.2	9
190	Strain and texture analysis of coatings using high-energy x-rays. Journal of Applied Physics, 2003, 94, 697-702.	1.1	103
191	Optimization of wear-resistant coating architectures using finite element analysis. Journal of Vacuum Science and Technology A: Vacuum, Surfaces and Films, 2003, 21, 332-339.	0.9	18
192	Characterisation of residual stress distribution in clinching joints of carbon steel by diffraction methods. Materials Science and Technology, 2003, 19, 336-342.	0.8	3
193	Growth of single-crystal CrN on MgO(001): Effects of low-energy ion-irradiation on surface morphological evolution and physical properties. Journal of Applied Physics, 2002, 91, 3589-3597.	1.1	117
194	Residual Stresses in a Nickel-Based Superalloy Introduced by Turning. Materials Science Forum, 2002, 404-407, 173-178.	0.3	36
195	Residual Stress Distributions around Clinched Joints. Materials Science Forum, 2002, 404-407, 617-622.	0.3	5
196	In situx-ray diffraction study ofC60polymerization at high pressure and temperature. Physical Review B, 2002, 66, .	1.1	26
197	Deformation structures under indentations in TiN/NbN single-crystal multilayers deposited by magnetron sputtering at different bombarding ion energies. Philosophical Magazine A: Physics of Condensed Matter, Structure, Defects and Mechanical Properties, 2002, 82, 1983-1992.	0.8	41
198	Thermal stability of arc evaporated high aluminum-content Ti1â^'xAlxN thin films. Journal of Vacuum Science and Technology A: Vacuum, Surfaces and Films, 2002, 20, 1815-1823.	0.9	314

#	Article	IF	CITATIONS
199	Influence of elastic and plastic anisotropy on the flow behavior in a duplex stainless steel. Metallurgical and Materials Transactions A: Physical Metallurgy and Materials Science, 2002, 33, 57-71.	1.1	57
200	Residual stress in clinched joints of metals. Applied Physics A: Materials Science and Processing, 2002, 74, s1440-s1442.	1.1	12
201	Intergranular strains and plastic deformation of an austenitic stainless steel. Materials Science & Engineering A: Structural Materials: Properties, Microstructure and Processing, 2002, 334, 215-222.	2.6	29
202	Deformation behaviour of a prestrained duplex stainless steel. Materials Science & Engineering A: Structural Materials: Properties, Microstructure and Processing, 2002, 337, 25-38.	2.6	37
203	Anisotropic High Cycle Fatigue Behaviour of Duplex Stainless Steels: Influence of Microstresses. International Journal of Materials Research, 2002, 93, 7-11.	0.8	5
204	Superhard and superelastic films of polymeric C60. Diamond and Related Materials, 2001, 10, 2044-2048.	1.8	18
205	Epitaxial NaCl structure Î-TaNx(001): Electronic transport properties, elastic modulus, and hardness versus N/Ta ratio. Journal of Applied Physics, 2001, 90, 2879-2885.	1.1	88
206	Microstructure, stress and mechanical properties of arc-evaporated Cr–C–N coatings. Thin Solid Films, 2001, 385, 190-197.	0.8	106
207	Growth, structure, and mechanical properties of transition metal carbide superlattices. Journal of Materials Research, 2001, 16, 1301-1310.	1.2	14
208	Mechanical and thermal stability of TiN/NbN superlattice thin films. Surface and Coatings Technology, 2000, 133-134, 227-233.	2.2	79
209	Microstructure–property relationships in arc-evaporated Cr–N coatings. Thin Solid Films, 2000, 377-378, 407-412.	0.8	44
210	Load sharing between austenite and ferrite in a duplex stainless steel during cyclic loading. Metallurgical and Materials Transactions A: Physical Metallurgy and Materials Science, 2000, 31, 1557-1570.	1.1	81
211	Microstructural evolution during tempering of arc-evaporated Cr–N coatings. Journal of Vacuum Science and Technology A: Vacuum, Surfaces and Films, 2000, 18, 121-130.	0.9	59
212	Micro- and Macrostress Evolution in a Duplex Stainless Steel during Uniaxial Loading. Materials Science Forum, 2000, 347-349, 603-608.	0.3	0
213	Growth and physical properties of epitaxial metastable cubic TaN(001). Applied Physics Letters, 1999, 75, 3808-3810.	1.5	65
214	Evolution of the residual stress state in a duplex stainless steel during loading. Acta Materialia, 1999, 47, 2669-2684.	3.8	163
215	Microstructure and mechanical behavior of arc-evaporated Cr–N coatings. Surface and Coatings Technology, 1999, 114, 39-51.	2.2	94
216	The effects of bias voltage and annealing on the microstructure and residual stress of arc-evaporated Cr–N coatings. Surface and Coatings Technology, 1999, 120-121, 272-276.	2.2	55

#	Article	IF	CITATIONS
217	Effect of laser hardening on the fatigue strength and fracture of a B–Mn steel. International Journal of Fatigue, 1998, 20, 389-398.	2.8	48
218	Influence of plasma nitriding on fatigue strength and fracture of a B-Mn steel. Materials Science & Engineering A: Structural Materials: Properties, Microstructure and Processing, 1998, 242, 181-194.	2.6	49
219	Characterization of the Induced Plastic Zone in a Single Crystal TiN(001) Film by Nanoindentation and Transmission Electron Microscopy. Journal of Materials Research, 1997, 12, 2134-2142.	1.2	64
220	Internal Stress in an Alumina/Silicon Carbide Whisker Composite. , 1997, , 391-403.		1
221	Nanoindentation studies of singleâ€crystal (001)â€, (011)â€, and (111)â€oriented TiN layers on MgO. Journal of Applied Physics, 1996, 80, 6725-6733.	1.1	239
222	Near-Surface Deformation in an Alumina-Silicon Carbide-Whisker Composite due to Surface Machining. Journal of the American Ceramic Society, 1996, 79, 2134-2140.	1.9	19
223	Internal Stress in an Alumina/Silicon Carbide Whisker Composite. Advances in X-ray Analysis, 1995, 39, 391-403.	0.0	1
224	Synthesis of Ti3SiC2 by Reaction of TiC and Si Powders. Ceramic Engineering and Science Proceedings, 0, , 21-30.	0.1	2
225	Free Standing AlN Single Crystal Grown on Pre-Patterned and <i>In Situ</i> Patterned 4H-SiC Substrates. Materials Science Forum, 0, 645-648, 1187-1190.	0.3	1
226	Deformation structures under indentations in TiN/NbN single-crystal multilayers deposited by magnetron sputtering at different bombarding ion energies. , 0, .		9
227	Synthesis and Phase Development in the Cr-Al-N System. Ceramic Engineering and Science Proceedings, 0, , 1-12.	0.1	0